Hydrogen Separation from Reforming Products by Silica Membrane: A Numerical Study

Davood Tahmasbi[1], Hassan Habibi Moghaddam[1]
[1]Department of Mechanical Engineering, Sahand University of Technology, Tabriz, Iran

Abstract— In this paper, a 2D axisymmetric computational fluid dynamics (CFD) model is presented for the process of hydrogen separation from reforming products by silica membrane. This model has the capability of showing selective permeance of species through membrane, as a preference to pervious works. In this work, effects of temperature, pressure difference, and feed inlet velocities on species molar fraction, silica membrane performance were investigated. For this purpose, ternary mixture of $H_2/CO_2/CO$ with percentages of 69/30/1 was chosen, and flow rate of 120 (mL/min) was considered as feed. As temperature increased from 323.15 K to 373.15 K, hydrogen molar fraction at the outlet of feed side decreased from 62.44 to 51.06, and at the outlet of permeate side, increased from 78.32 to 80.82. Increase in pressure difference led to reduction of molar fraction for hydrogen and increase for other components at permeate side. At retentate side, hydrogen molar fraction was reduced with pressure difference rise, from 1 to 3 bar, while for 3 to 4 bar it increased. Increasing the feed inlet velocity from 5.99 to 8.29 mm/s resulted in hydrogen molar fraction rise from 30.17 to 37.71 at retentate side and from 77.03 to 82.52 at permeate side. Therefore, silica membrane operated more effectively at higher temperatures, lower pressure differences, and mean velocities.

Keywords— CFD simulation, Hydrogen separation, Reforming products, Silica membrane.

I. INTRODUCTION

Hydrogen is known as a clean energy source [1] which has been used for power production and heating. It is also a key element of fuel cells [2]. A method for hydrogen production is reforming of natural gas which is economically profitable [2]. Reforming gas products generally include hydrogen, carbon monoxide, and carbon dioxide [3, 4]. Poisonous effects of carbon monoxide is one of the reasons that it should be removed from reforming gas products [5]. Another important product of reforming process is carbon dioxide which is known as the most challenging greenhouse gas [6-8], hence, its separation is really important and it should be prevented from releasing into the atmosphere [6]. Considering these points, separation process of these species has attracted a lot of attention these days. Membrane technology is one of the gas separation methods which uses low energy [9, 10]. This technology has been widely used in membrane reactors which are a common system for hydrogen production by reforming process. Hydrogen production from ammonia decomposition was modeled by Chein et al. [11]. Moreover, a mathematical model was developed for steam reforming in a membrane reactor [12-14]. In another work, a bench-scale membrane module of hydrogen selective Pd-based composite membrane was used to investigate the CO_2 capture [15]. Ghasemzadeh et al. [16] analyzed the operation of a silica membrane reactor for carrying out the methanol steam reforming reaction for

hydrogen production. Analysis of reforming process in membrane reactor requires good knowledge about membrane behavior. For this purpose, a CFD model for H_2 selective extraction from H_2/CO gas mixture using a ceramic membrane, e.g. porous silica membrane, in the steam reforming process was developed by Takaba and Nakao [17]. Barbieri et al. [18] analyzed hydrogen permeation through Pd-Ag membranes to determine a quantitative relationship describing the dilution and inhibition effects. Also, a comprehensive two dimensional validated model for carbon dioxide transport using hollow fiber membrane (HFM) was presented by Al-Marzouqi et al. [19, 20].

Shirazian et al. [21] simulated mass transfer for gas-liquid contactor membrane by a model in which momentum and mass transfer equations were solved in a hollow fiber membrane contactor for laminar flow conditions. Rezakazemi et al. [22] studied H_2S and CO_2 chemical absorption from natural gas by hollow fiber membranes. Experimental and simulation results indicated that the membrane module was very efficient in H_2S trace removal at high gas/liquid flow ratio. Absorption of carbon dioxide in hollow fiber membrane contactors (HFMC) has been modeled mathmatically [23]. A two-dimensional numerical method was presented by Chen et al. [24] to simulate the phenomena of concentration polarization for hydrogen permeation in a Pd-based membrane tube. In brief, it is concluded that the H_2 permeation rate can be predicted by Sieverts' law if the H_2 permeation ratio isn't larger than 30%. Boon et al. [25] employed a combination of experimental work and numerical simulation in order to investigate different palladium membrane layers parts from overall resistance against mass transfer through the membrane. Considering solvent evaporation, Ghasem et al. [26] developed a model for CO_2 absorption in a membrane contactor. Amooghin et al. [27] presented a mathematical model of mass transfer in multicomponent gas mixture across the synthesized composite polymeric membrane. Zhang et al. evaluated effect of geometrical parameters such as fibers inner radios, membrane thickness and module inner radios on carbon dioxide absorption [28]. Coroneo et al. [29] investigated the performances of inorganic membrane modules for gas mixture separation using a model in which the membrane was modeled as a selective layer that allows the permeation of different components as a function of the transport mechanism and driving force. Investigation of membrane operating condition has been mentioned by some athours as another important subject in this field. Abdel-Jawad et al. [30] showed the effect of flow condition on single gas diffusion in both zones of feed/retentate and permeate using

silica membrane and activated gas transport model. Katoh et al. [31] evaluated the computational results of a dynamic simulation to compare the effect of mixing degree in the feed side and permeate side. This was done for the process of multicomponent gas separation by hollow-fiber membrane module. Shehni et al. [32] established a model for unsteady-state permeation of gas mixture through a self-synthesized PDMS membranes which predicted permeation behavior of pure and mixed gases at different operating conditions. The impact of operating conditions on the performance of a multi-tube membrane module containing cobalt oxide silica membranes with molecular sieving properties was investigated by Wang et al. [33]. Kárászová et al. [34] studied the effects of temperature and stage cut on permeation of CO_2 and CH_4 through two different supported liquid membrane.

Nevertheless, there are only a few CFD works reported in the literature which have modeled gas-through-gas diffusion through silica membranes. Moreover, lack of a comprehensive model for transportation of species with an average diameter close to diameter of the membrane pores could be sensed. This study used numerical analysis to represent a useful guide to improve researchers' view about these kinds of membranes. Numerical analysis has been used in various areas [35-42]. The primary aim of the present work is to investigate CO, CO_2, and H_2 simultaneous transfer and separation process using a silica membrane by an axisymmetric two dimensional model. In this model, momentum and mass transfer equations are coupled and solved simultaneously for feed and permeate sides. This coupling was achieved using velocity, density and mixture viscosity. The membrane is considered as a wall without thickness. Then, the sink and source terms were applied in order to consider species transportation through silica membrane using their local driving force. This driving force has been taken into account in terms of molecular sieve activated mechanism as the governing transport mechanism. Results of this model were validated against experimental data which have been measured in Nanostructure Material Research Center of Sahand University of Technology (NMRC of SUT). Finally, performance of silica membrane at different operational conditions has been studied.

II. MATERIAL AND METHODS

A. Governing Equations

Governing equation of the mathematical model was developed by a material balance on the silica membrane layer. The computational domain of the permeation system is shown in Fig. 1 schematically. To make the model simpler and reduce calculation time, the 2-D geometry can be obtained from the real 3–D geometry under the hypothesis of axial symmetry. Modeling of these processes includes three sides of feed, membrane and permeate. Gas mixture enters the feed side at z = 0 and accumulates on the membrane surface. Then, based on passing mechanism, some parts of gas molecules pierce through membrane selectively and enter the permeate side. Finally, non- pierced molecules exit as retentate flow. In this model, membrane was considered as a wall without

thickness. For taking the mass transfer into account, sink and source terms were employed in both membrane sides.
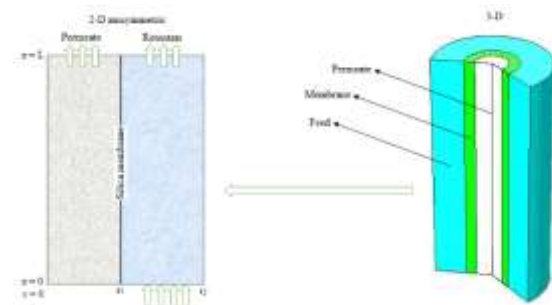

Fig. 1. Model domain considered in the silica membrane module consisting of the feed, membrane and permeate sides, $r_1 = 5$ mm, $r_2 = 11$ mm, L = 50 mm.

Modeling assumptions:
1. Separation process is done isothermally in steady state condition.
2. Flow regime in both sides of feed and permeate is laminar.
3. The gas mixture is considered as ideal gas.
4. The absence of chemical reaction in the system.
5. Total pressure of both feed and permeate sides are constant.
6. Steam effect on silica membrane is negligible.
7. The film transport resistance supposed at the interface gas/membrane was considered negligible.

In this membrane system, mass and momentum transfer equations in both feed and permeate sides were modeled using Navier–Stokes equations, species conservation and ideal gas equation of state. These equations were coupled to each other by terms such as mixture density and viscosity and velocity as common terms of Navier–Stokes and species conservation equations [43].

1. Continuity equation
$$\nabla.\rho V = S \tag{1}$$

2. Momentum equation
$$\rho V.\nabla V = -\nabla P + \nabla.\left[\mu\left(\nabla V + \left(\nabla V\right)^T\right)\right] \tag{2}$$

3. Chemical species conservation equation
$$\nabla. C_i V = \nabla\left(D_{ij}\ \nabla C_i\right) + S_i \tag{3}$$

4. Ideal gas equation of state
$$P = \rho RT\sum_{i}^{N}\frac{1}{x_i M_i} \tag{4}$$

In which, ρ is mixture density, V velocity, S source term, P total pressure, μ viscosity, R universal gas constant, T temperature, C_i concentration of component i, D_{ij} diffusion coefficient of any component in the gas phase, x_i molar fraction of component i and M_i molar mass of component i.

B. Properties of Gas Mixture

In order to calculate gas mixture density, ideal gas equation of state could be used, if an ideal gas mixture has been considered. For calculation of viscosity and diffusion coefficient some correlations should be employed. Viscosity of mixture could be calculated by Wilke semi-empirical equation as follows [44].

$$\mu_{mix} = \frac{\sum x_i \mu_i}{\sum x_i \phi_{i,j}} \qquad (5)$$

$$\phi_{i,j} = \frac{1}{2\sqrt{2}} (1 + M_i / M_j)^{-0.5} \left[1 + (\mu_i / \mu_j)^{0.5} (M_j / M_i)^{0.25} \right]^2 \qquad (6)$$

Where μ_i is viscosity of component i and M_j molar mass of component j, which could be found in table I [45]. Diffusion coefficients of any component in the gas phase, could be calculated by Chapman-Enskog equation as follows[46].

$$D_{ij} = \frac{1.86 \times 10^{-3} T^{1.5} \left(1/M_i + 1/M_j \right)^{.5}}{P \sigma_{ij}^2 \Omega} \qquad (7)$$

In which, M_j is molar mass of component j, σ_{ij} is interaction value for binary mixture and Ω is diffusion collision integral. All parameters are given in TABLE I.

TABLE I. Model parameters [45,46].

Parameter	Value
σ_{H_2}	2.827 (A)
σ_{CO_2}	3.941 (A)
σ_{CO}	3.69 (A)
$\Omega_{H_2-CO_2}$	0.86604
Ω_{H_2-CO}	0.803508
Ω_{CO-CO_2}	0.90983
M_{H_2}	2 (g mol^{-1})
M_{CO_2}	44 (g mol^{-1})
M_{CO}	28 (g mol^{-1})
μ_{H_2}	1.75×10^{-5} (Pa. s)
μ_{CO_2}	2.7×10^{-5} (Pa. s)
μ_{CO}	1.47×10^{-5} (Pa. s)

C. Boundary Conditions

Gas mixture enters the feed side at z = 0 with specified concentration and velocity. Then, based on activated molecular sieve diffusion mechanism, species permeate from membrane boundary at r = r1. In order to describe species permeation flux at this boundary, the sink and source terms were used. This system includes two outlets at z = L for feed and permeate sides which have been described as pressure outlet boundary condition for Navier–Stokes equations and as zero concentration gradient for species conservation equation. Then, due to symmetry geometry of the problem, axisymmetric boundary condition was employed at z = 0 and r = 0. Finally at r = r2, no slip boundary condition was considered for Navier–Stokes equations and zero gradient for spices conservation equations [47, 48].

The silica membrane was synthesized on the modified support via sol-gel method by Ghasemzadeh et al. [39] due to high stability and quality of the modified γ-alumina support. The permeations tests were done by stainless steel module in NMRC of SUT. Data represented in table II are values related to pre-exponential coefficient of permeance and activation

energy of components. These values have been achieved by curve fitting of permeation values [47, 48].

TABLE III. Silica membrane properties [47, 48]

Gas	$Pe_{0,i}^*$ (mol m^{-2} s^{-1} Pa^{-1})	$E_{a,i}$ (kJmol^{-1})
H$_2$	1.563×10^{-5}	9.999
CO$_2$	1.881×10^{-8}	-5.260
CO	7.06×10^{-8}	5.33

A. CFD Simulation

In order to solve the model equations related to feed, membrane and permeate zones with appropriative boundary conditions, COMSOL software was employed. This finite element based commercial software analyzes with a combined mapped and boundary layer which has been used by scientists to solve numerical problems in various areas such as fluid dynamics, heat transfer, and biomechanics [49, 50]. To control error, a variety of numerical solvers such as PARDISO were used. Run simulation conducted by a personal computer with an Intel(R) core(TM) i7-4500U CPU @ 1.80GHz-2.4GHz and 8GB RAM.

III. RESULTS AND DISCUSSION

A. Model Validation

In this work, the validation of the model was accomplished using experimental data which was obtained in NMRC of SUT from experiments on a synthesis silica membrane for different mixtures and operational conditions. For 75/25 mixture of H$_2$/CO$_2$ and 99/1 mixture of H$_2$/CO which will be called as "1st combination" and "2nd combination" respectively, membrane operational conditions are given in table III and table IV. At these conditions, predicted and experimental mean values of hydrogen molar fraction in outlet of feed (retentate) and permeate sides are compared in Fig. 2 and 3 which show a good agreement between them.

TABLE III. Membrane operational condition for 1st combination (T = 473 K).

Flow rate in permeate flow (mL/min)	Flow rate in retentate flow (mL/min)	Pressure difference (bar)
230	120	2
610	130	4

TABLE IV. Membrane operational condition for 2nd combination (T=473K).

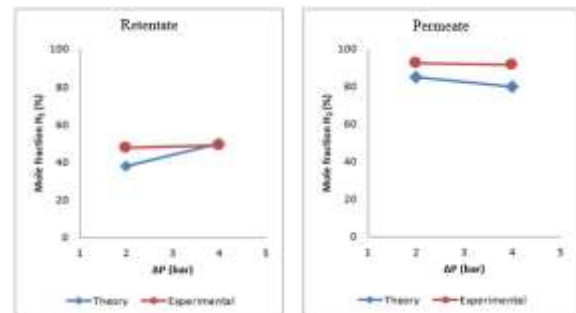| Flow rate in permeate flow (mL/min)	Flow rate in retentate flow (mL/min)	Pressure difference (bar)
235	135	2
615	135	4

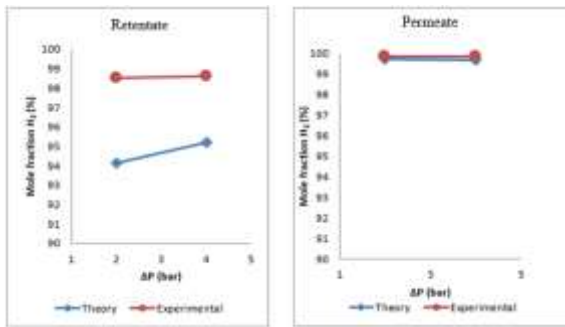Fig. 2. Mean values of hydrogen molar fraction in retentate and permeate sides for 1st combination.

Fig. 3. Mean values of hydrogen molar fraction in retentate and permeate sides for 2nd combination.

B. Mesh Independency

In order to be sure that model results are independent from mesh numbers, hydrogen molar fraction in outlet of feed and permeate sides was calculated while mesh numbers increased gradually. Results reported in table V suggest that the difference between the second and the third grid systems is almost imperceptible. As a consequence, 51076 elements have been employed for modeling in this work.

TABLE V. Mesh independency.

# of elements	H_2 molar fraction in retentate	H_2 molar fraction in permeate	% Difference Retentate	Permeate
13160	32.19	78.81	-	-
31055	32.22	78.87	0.09	0.07
51076	32.23	78.91	0.03	0.05

C. Species Molar Fraction in Feed and Permeated Sides

To provide a clear observation of species concentration, Fig. 4 depicts contour of species molar fraction variation in both radial and axial directions in membrane module for $H_2/CO_2/CO$ combination. The variation of molar fraction in permeate side is small while in the feed side, a sharp decrease in molar fraction of each component can be found. The reason of this behavior was that diffusion coefficients in the permeate side were 3 order of magnitude larger compared to the feed side. Therefore, in the feed side, hydrogen was a selective specie which its molar fraction has been reduced in radial and axial directions while other species molar fractions have been increased. At the first steps of species transfer through membrane, hydrogen had the most diffusion in comparison with other species due to its tendency to permeate which was the consequence of having the most driving force. As time passes, this driving force was reduced on the contrary of its increase for other species. Hence, molar fraction variation in permeate side showed reduction for selective specie and increase for other species.

D. Velocity Profile

Upon inspection of gas velocity variation, data for velocity profiles of the gas phases in two compartments (feed and permeate sides) presented in Fig. 5. According to correlation (8) from [37], longest development length possible in feed side in which boundary layers meet each other had little values (L_e = 0.000008-0.00001 m).
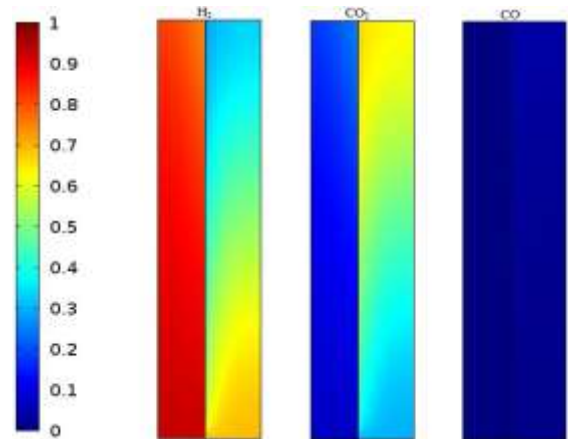
$$L_e/D = 0.04Re \tag{8}$$

Where D is (r_2-r_1).

Fig. 4. Species molar fractions in membrane module for $H_2/CO_2/CO$ combination, Flow rate in feed = 120 (mL/min), T = 473 K, ΔP = 2 bar.

With a little distance from feed side entrance, velocity profile was fully developed and reached to its maximum value. Then, stream wise velocity was reduced due to mass transfer through membrane. For permeate side, absence of sweep gas introduced zero velocity at the entrance which was at its lowest value. Then, it increased by increment of mass transfer through membrane and reached to its highest value at outlet of this side.
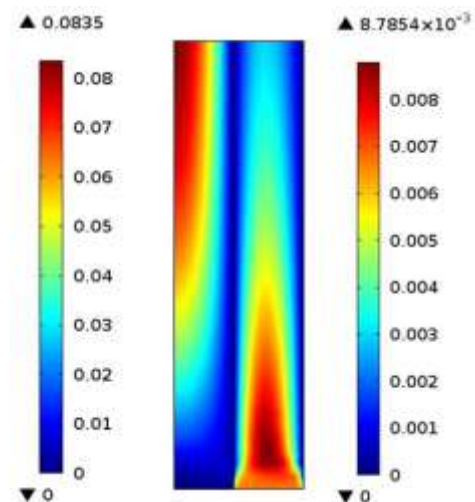

Fig. 5. Velocity contours for $H_2/CO_2/CO$ combination at the condition of T = 473 K, ΔP = 2 bar, flow rate of feed = 120 (mL/min).

E. Silica Membrane Performance

Criterion to evaluate operation of silica membrane for hydrogen separation was hydrogen molar fraction values at both retantate and permeate sides. For this purpose, species molar fraction variation indicated by parameters such as pressure difference, temperature and feed inlet velocity was evaluated at these sides. Ternary mixture of $H_2/CO_2/CO$ with percentages of 69/30/1 were chosen and a flow rate of 120 (mL/min) was considered as feed. The effect of pressure difference on the mole fractions of species in feed and permeate sides is shown in Fig. 6 and 7. Increase in pressure

236

difference led to reduction of molar fraction for hydrogen and increase for other components at permeate side. At retentate side, hydrogen molar fraction was reduced with pressure difference rise, from 1 to 3 bar, while for 3 to 4 bar it increased and permeation rate was reduced due to reduction of hydrogen partial pressure difference.
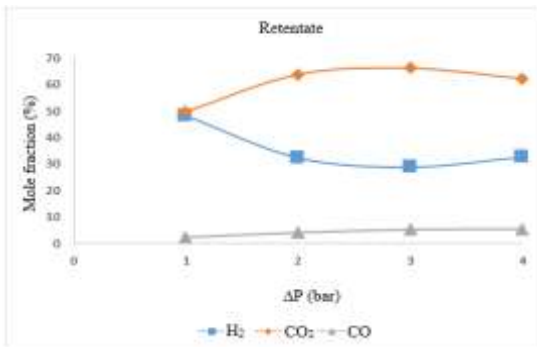

Fig. 6. Molar fraction variation of $H_2/CO_2/CO$ mixture components, depending on the pressure difference in retentate side at T = 473 K.
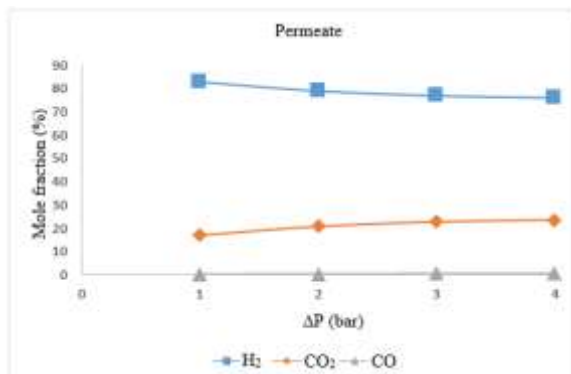

Fig. 7. Molar fraction variation of $H_2/CO_2/CO$ mixture components, depending on the pressure difference in permeate side at T = 473 K.

Temperature is another parameter influencing silica membrane operation. According to molecular sieve mechanism, permeability is an exponential function of temperature. Permeance pre-exponential coefficient and activation energy are basic parameters of this function. According to table II, activation energy of hydrogen has a positive sign and its kinetic diameter is smaller than other species. With temperature rise, permeability of species with positive activation energy increased. Therefore, according to molecular sieve activated mechanism, selective specie (hydrogen) permeated with more and other species with less tendency. As could be seen in Fig. 8 and 9, with temperature rise from 323.15 K to 373.15 K, hydrogen molar fraction at retentate side decreased from 62.44 to 51.06 and in permeate flow, rised from 78.32 to 80.82. Despite of positive sign of carbon monoxide activation energy, its permeability was descending due to its bigger kinetic diameter and lower propulsion. The activation energy of carbon dioxide has negative sign, hence, with temperature rise, the gas permeability was reduced.

The effect of feed inlet velocities on the species separation is shown in Fig. 10 and 11. As expected, increase in feed inlet velocity reduced the residence time of gas mixture at feed side, and consequently reduction of permeation rate.
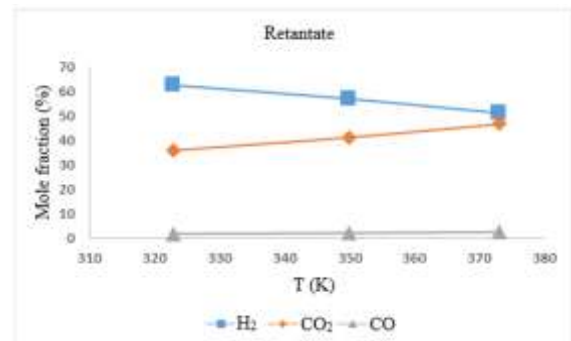

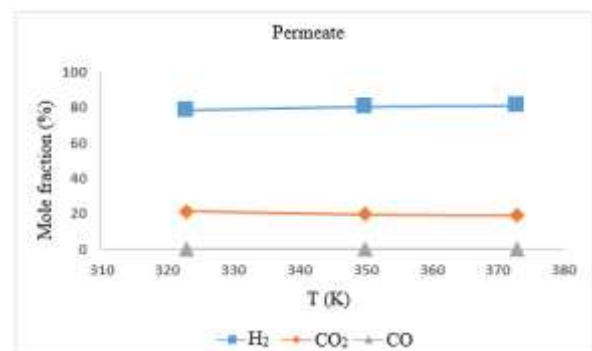Fig. 8. Molar fraction variation of $H_2/CO_2/CO$ mixture components, depending on the temperature in retentate side with $\Delta P = 2$ bar.

Fig. 9. Molar fraction variation of $H_2/CO_2/CO$ mixture components, depending on the temperature in permeate side with $\Delta P = 2$ bar.
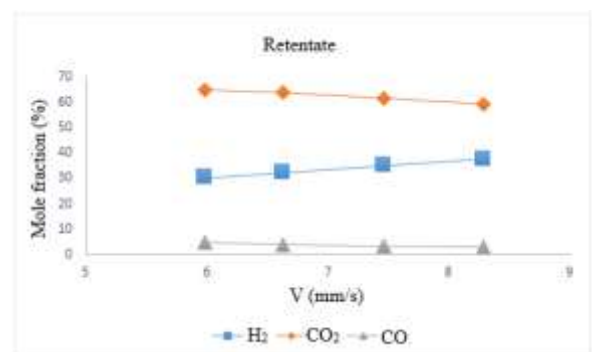

Fig. 10. Variation of mixture components molar fraction in $H_2/CO_2/CO$ mixture, depending on the gas velocity in retentate side with $\Delta P = 2$ bar.
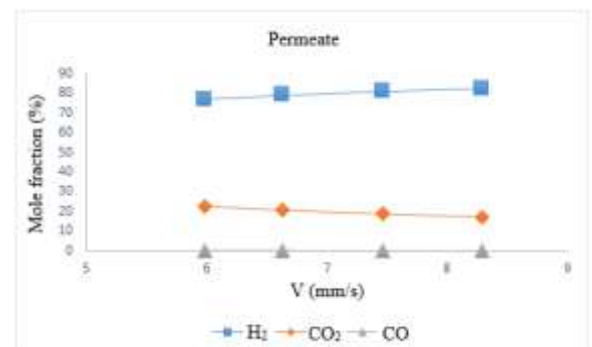

Fig. 11. Molar fraction variation of $H_2/CO_2/CO$ mixture components, depending on the gas velocity in permeate side with $\Delta P = 2$ bar.

So, increasing the feed inlet velocity from 5.99 to 8.29 mm/s, resulted in hydrogen molar fraction rise from 30.17 to 37.71 at retentate side and from 77.03 to 82.52 at permeate side. This happened while other gases molar fraction was reduced at both sides. It can be concluded that as the feed inlet velocity increased, hydrogen purification increased at permeate side and other components concentration was reduced at retentate side.

IV. CONCLUSION

In this work, an axisymmetric two dimensional model was employed for CFD analysis of silica membrane. Using this model, velocity and concentration profiles of species were presented in feed and permeate sides. Evaluation of silica membrane performance at different temperature, pressure difference and gas velocities was performed using ternary mixture of $H_2/CO_2/CO$ with gases percentage of 69/30/1. Both concentration and purity of hydrogen increased at permeate side with temperature rise. Therefore, temperature has direct relation with hydrogen permeability, and silica membrane is more effective in high temperatures. The next parameter is pressure difference between feed and permeate sides. Hydrogen separation can be done better in a silica membrane with lower pressure difference. With increase in feed inlet velocity hydrogen purification increased at permeate side and other components concentration was reduced at retentate side. Consequently, silica membrane has its optimized operation of hydrogen separation in high temperature, low pressure difference and average velocity.

REFERENCES

[1] Gopalakrishnan S, da Costa JCD. Hydrogen gas mixture separation by CVD silica membrane. Journal of Membrane Science, 323:144-7, (2008).

[2] Brunetti A, Drioli E, Lee YM, Barbieri G. Engineering evaluation of CO2 separation by membrane gas separation systems. Journal of Membrane Science, 454:305-15, (2014).

[3] Ye J, Yang J, Zheng J, Ding X, Wong I, Li W, et al. A multi-scale flow analysis in hydrogen separation membranes using a coupled DSMC-SPH method. International Journal of Hydrogen Energy, 37:894-902, (2012).

[4] Ghasemzadeh K, Liguori S, Morrone P, Iulianelli A, Piemonte V, Babaluo A, et al. H 2 production by low pressure methanol steam reforming in a dense Pd–Ag membrane reactor in co-current flow configuration: Experimental and modeling analysis. International Journal of Hydrogen Energy, 38:16685-97, (2013).

[5] Ghasemzadeh K, Morrone P, Liguori S, Babaluo A, Basile A. Evaluation of silica membrane reactor performance for hydrogen production via methanol steam reforming: Modeling study. International Journal of Hydrogen Energy, 38:16698-709, (2013).

[6] Kangas J, Sandström L, Malinen I, Hedlund J, Tanskanen J. Maxwell–Stefan modeling of the separation of H2 and CO2 at high pressure in an MFI membrane. Journal of Membrane Science, 435:186-206, (2013).

[7] Chen HZ, Thong Z, Li P, Chung T-S. High performance composite hollow fiber membranes for CO2/H2 and CO2/N2 separation. International Journal of Hydrogen Energy, 39:5043-53, (2014).

[8] Ahmadpour E, Shamsabadi AA, Behbahani RM, Aghajani M, Kargari A. Study of CO2 separation with PVC/Pebax composite membrane. Journal of Natural Gas Science and Engineering, 21:518-23, (2014).

[9] Khalilpour R, Abbas A, Lai Z, Pinnau I. Analysis of hollow fibre membrane systems for multicomponent gas separation. Chemical Engineering Research and Design, 91:332-47, (2013).

[10] Dorosti F, Omidkhah M, Abedini R. Enhanced CO2/CH4 separation properties of asymmetric mixed matrix membrane by incorporating nano-porous ZSM-5 and MIL-53 particles into Matrimid® 5218. Journal of Natural Gas Science and Engineering, 25:88-102, (2015).

[11] Chein R-Y, Chen Y-C, Chang C-S, Chung J. Numerical modeling of hydrogen production from ammonia decomposition for fuel cell applications. International Journal of Hydrogen Energy, 35:589-97, (2010).

[12] Iulianelli A, Manzolini G, De Falco M, Campanari S, Longo T, Liguori S, et al. H 2 production by low pressure methane steam reforming in a Pd–Ag membrane reactor over a Ni-based catalyst: experimental and modeling. International Journal of Hydrogen Energy, 35:11514-24, (2010).

[13] Gallucci F, De Falco M, Tosti S, Marrelli L, Basile A. Ethanol steam reforming in a dense Pd–Ag membrane reactor: a modelling work. Comparison with the traditional system. International Journal of Hydrogen Energy, 33:644-51, (2008).

[14] Said SA, Simakov DS, Mokheimer EM, Habib MA, Ahmed S, Waseeuddin M, et al. Computational fluid dynamics study of hydrogen generation by low temperature methane reforming in a membrane reactor. International Journal of Hydrogen Energy, 40:3158-69, (2015).

[15] Ryi S-K, Park J-S, Hwang K-R, Lee C-B, Lee S-W. The property of hydrogen separation from CO2 mixture using Pd-based membranes for carbon capture and storage (CCS). International Journal of Hydrogen Energy, 38:7605-11, (2013).

[16] Ghasemzadeh K, Morrone P, Babalou A, Basile A. A simulation study on methanol steam reforming in the silica membrane reactor for hydrogen production. International Journal of Hydrogen Energy, 40:3909-18, (2015).

[17] Takaba H, Nakao Si. Computational fluid dynamics study on concentration polarization in H2/CO separation membranes. Journal of membrane science, 249:83-8, (2005).

[18] Barbieri G, Scura F, Lentini F, De Luca G, Drioli E. A novel model equation for the permeation of hydrogen in mixture with carbon monoxide through Pd–Ag membranes. Separation and Purification technology, 61:217-24, (2008).

[19] Al-Marzouqi MH, El-Naas MH, Marzouk SA, Al-Zarooni MA, Abdullatif N, Faiz R. Modeling of CO2 absorption in membrane contactors. Separation and Purification Technology, 59:286-93, (2008).

[20] Al-Marzouqi M, El-Naas M, Marzouk S, Abdullatif N. Modeling of chemical absorption of CO2 in membrane contactors. Separation and Purification Technology, 62:499-506, (2008).

[21] Shirazian S, Moghadassi A, Moradi S. Numerical simulation of mass transfer in gas–liquid hollow fiber membrane contactors for laminar flow conditions. Simulation Modelling Practice and Theory, 17:708-18, (2009).

[22] Rezakazemi M, Niazi Z, Mirfendereski M, Shirazian S, Mohammadi T, Pak A. CFD simulation of natural gas sweetening in a gas–liquid hollow-fiber membrane contactor. Chemical Engineering Journal, 168:1217-26, (2011).

[23] Saidi M, Heidarinejad S, Rahimpour HR, Talaghat MR, Rahimpour MR. Mathematical modeling of carbon dioxide removal using amine-promoted hot potassium carbonate in a hollow fiber membrane contactor. Journal of Natural Gas Science and Engineering, 18:274-85, (2014).

[24] Chen WH, Syu WZ, Hung CI. Numerical characterization on concentration polarization of hydrogen permeation in a Pd-based membrane tube. International Journal of Hydrogen Energy, 36:14734-44, (2011).

[25] Boon J, Pieterse J, Dijkstra J, van Sint Annaland M. Modelling and systematic experimental investigation of mass transfer in supported palladium-based membrane separators. International Journal of Greenhouse Gas Control, 11:S122-S9, (2012).

[26] Ghasem N, Al-Marzouqi M, Rahim NA. Modeling of CO2 absorption in a membrane contactor considering solvent evaporation. Separation and Purification Technology, 110:1-10, (2013).

[27] Amooghin AE, Shehni PM, Ghadimi A, Sadrzadeh M, Mohammadi T. Mathematical modeling of mass transfer in multicomponent gas mixture across the synthesized composite polymeric membrane. Journal of Industrial and Engineering Chemistry, 19:870-85, (2013).

[28] Zhang Z, Yan Y, Zhang L, Chen Y, Ju S. CFD investigation of CO2 capture by methyldiethanolamine and 2-(1-piperazinyl)-ethylamine in

membranes: Part B. Effect of membrane properties. Journal of Natural Gas Science and Engineering, 19:311-6, (2014).

[29] Coroneo M, Montante G, Giacinti Baschetti M, Paglianti A. CFD modelling of inorganic membrane modules for gas mixture separation. Chemical Engineering Science, 64:1085-94, (2009).

[30] Abdel-Jawad M, Gopalakrishnan S, Duke M, Macrossan M, Schneider PS, Diniz da Costa J. Flowfields on feed and permeate sides of tubular molecular sieving silica (MSS) membranes. Journal of Membrane Science, 299:229-35, (2007).

[31] Katoh T, Tokumura M, Yoshikawa H, Kawase Y. Dynamic simulation of multicomponent gas separation by hollow-fiber membrane module: Nonideal mixing flows in permeate and residue sides using the tanks-in-series model. Separation and Purification Technology, 76:362-72, (2011).

[32] Shehni PM, Amooghin AE, Ghadimi A, Sadrzadeh M, Mohammadi T. Modeling of unsteady-state permeation of gas mixture through a self-synthesized PDMS membranes. Separation and Purification Technology, 76:385-99, (2011).

[33] Ji G, Wang G, Hooman K, Bhatia S, da Costa JCD. Simulation of binary gas separation through multi-tube molecular sieving membranes at high temperatures. Chemical Engineering Journal, 218:394-404, (2013).

[34] Kárászová M, Sedláková Z, Friess K, Izák P. Effective permeability of binary mixture of carbon dioxide and methane and pre-dried raw biogas in supported ionic liquid membranes. Separation and Purification Technology, 153:14-8, (2015).

[35] Joukar, Amin, Hanieh Niroomand-Oscuii, and Farzan Ghalichi. "Numerical simulation of osteocyte cell in response to directional mechanical loadings and mechanotransduction analysis: Considering lacunar–canalicular interstitial fluid flow." Computer Methods and Programs in Biomedicine 133: 133-141 (2016).

[36] Gupta, Anil Kumar, Amin Joukar, Ryan O'Connell, and Vijay K. Goel. "The Evaluation of Shoulder Abduction with and without Rotation on the Supraspinatus Tendon and Labrum: A Finite Element Study." Orthopaedic Journal of Sports Medicine 5, no. 7_suppl6: 2325967117S00380 (2017).

[37] Walvekar, Aditya A., Dallin Morris, Zamzam Golmohammadi, Farshid Sadeghi, and Martin Correns. "A Novel Modeling Approach to Simulate Rolling Contact Fatigue and Three-Dimensional Spalls." Journal of Tribology 140, no. 3: 031101 (2018).

[38] Morris, Dallin, Zamzam Golmohammadi, Farshid Sadeghi, and Martin Correns. "A Novel Modeling Approach to Simulate Rolling Contact Fatigue and Three-Dimensional Spalls."

[39] Joukar, Amin, Jwalant Mehta, David Marks, and Vijay K. Goel. "Lumbar-Sacral Destruction Fixation Biomechanics: A Finite Element Study." The Spine Journal 17, no. 11: S335 (2017).

[40] Ahmadi, Arman, Reza Mirzaeifar, Narges Shayesteh Moghaddam, Ali Sadi Turabi, Haluk E. Karaca, and Mohammad Elahinia. "Effect of manufacturing parameters on mechanical properties of 316L stainless steel parts fabricated by selective laser melting: A computational framework." Materials & Design 112 (2016): 328-338.

[41] Ahmadi, Arman, Narges Shayesteh Moghaddam, Mohammad Elahinia, Haluk E. Karaca, and Reza Mirzaeifar. "Finite element modeling of selective laser melting 316l stainless steel parts for evaluating the mechanical properties." In ASME 2016 11th International Manufacturing Science and Engineering Conference, pp. V002T01A003-V002T01A003. American Society of Mechanical Engineers, 2016.

[42] Joukar, Amin, Anoli Shah, Ali Kiapour, Ardalan Seyed Vosoughi, Bradley Duhon, Anand K. Agarwal, Hossein Elgafy, Nabil Ebraheim, and Vijay K. Goel. "Gender Specific Sacroiliac Joint Biomechanics During Standing Upright: A Finite Element Study." Spine (2018).

[43] Chen W-H, Syu W-Z, Hung C-I, Lin Y-L, Yang C-C. A numerical approach of conjugate hydrogen permeation and polarization in a Pd membrane tube. International Journal of Hydrogen Energy, 37:12666-79, (2012).

[44] Caravella A, Barbieri G, Drioli E. Modelling and simulation of hydrogen permeation through supported Pd-alloy membranes with a multicomponent approach. Chemical Engineering Science, 63:2149-60, (2008).

[45] White FM. Fluid mechanics, WCB. ed: McGraw-Hill, Boston. (1999)

[46] Treybal RE, Treybal Robert E. Mass-transfer operations: McGraw-Hill New York. (1968).

[47] Aghaeinejad-Meybodi A, Ghasemzadeh K, Babaluo AA, Morrone P, Basile A. Modeling study of silica membrane performance for hydrogen separation. Asia-Pacific Journal of Chemical Engineering, (2015).

[48] Ghasemzadeh K, Aghaeinejad-Meybodi A, Vaezi MJ, Gholizadeh A, Abdi MA, Babaluo AA, et al. Hydrogen Production via Silica Membrane Reactor during Methanol Steam Reforming Process: Experimental Study. RSC Advances, (2015).

[49] Joukar A, Nammakie E, Niroomand-Oscuii H. A comparative study of thermal effects of 3 types of laser in eye: 3D simulation with bioheat equation. Journal of Thermal Biology, 49:74-81, (2015).

[50] Dede EM. Multiphysics topology optimization of heat transfer and fluid flow systems. In proceedings of the COMSOL Users Conference, (2009).

239